AIP Applied Physics Letters

# Space–time digital holography: A three-dimensional microscopic imaging scheme with an arbitrary degree of spatial coherence

Guy Indebetouw and Prapong Klysubun

Citation: Applied Physics Letters **75**, 2017 (1999); doi: 10.1063/1.124901

View online: http://dx.doi.org/10.1063/1.124901

View Table of Contents: http://scitation.aip.org/content/aip/journal/apl/75/14?ver=pdfcov

Published by the AIP Publishing

# Space–time digital holography: A three-dimensional microscopic imaging scheme with an arbitrary degree of spatial coherence

Guy Indebetouw[a] and Prapong Klysubun
*Department of Physics, Virginia Tech, Blacksburg, Virginia 24061-0435*

(Received 1 July 1999; accepted for publication 9 August 1999)

An on-line, spatiotemporal, digital holographic method is described and demonstrated experimentally. Using interferometric imaging, each scatterer of a three-dimensional object is encoded as a temporally modulated Fresnel pattern, and recorded on a charge-coupled device. Temporal heterodyning of the signal from each pixel results in a single-sideband, on-line holographic record in digital form. Reconstruction of an image focused on a chosen transverse plane in the object is done by digital correlation with a reconstruction function matched to that plane. The method circumvents most of the drawbacks of both coherent and incoherent holography, and may find applications in three-dimensional imaging and microscopy. © *1999 American Institute of Physics.* [S0003-6951(99)04640-9]

Holography has been used for the three-dimensional (3D) imaging of dilute collections of scatterers such as encountered in particle field analyses, and for the standard as well as interferometric imaging of three-dimensional (3D) objects.[1,2] Recent advances in high resolution spatial sensors, such as charge-coupled devices (CCD), has prompted the reassessment, in the new context of digital holography, of several original ideas that had emerged from the seminal work of Gabor[3] and Leith.[4] Digital holography refers to holographic methods that use solid-state detectors (such as CCDs), and store the hologram in digital form. Microscopy was the original goal of holography.[3,5] Conventional holograms are recorded interferometrically in the spatial domain, and reconstructed by spatial heterodyning,[4] thus requiring high degrees of both spectral and spatial coherence. In applications requiring high resolution imaging, spatial coherence has the disastrous consequence of producing images corrupted by the ubiquitous speckle noise.[6] Speckles have an average size equal to the resolution limit, and thus irrevocably mask the finer details of the image. This has been one of the main reasons for the relative lack of success of coherent holographic microscopy. Nevertheless, the main attraction of holographic imaging is that 3D data are acquired in a single shot, in contrast to other 3D imaging methods requiring multiple sequential scans. To overcome the problems due to coherence, and to permit holographic recording of self-luminous and fluorescent objects, incoherent methods have been proposed.[7] Most incoherent holographic schemes, however, are rather impractical because of their extremely poor signal-to-background ratio. This problem can also be traced to the fact that the holographic information exists in the spatial domain.

Much of these difficulties can be alleviated if the holographic data are recorded in the temporal domain, and reconstructed by temporal heterodyning, rather than spatial heterodyning. If spatial heterodyning is not needed, there is no need for spatial coherence, and the speckle problem disappears. Furthermore, temporal heterodyning is designed to extract a weak signal from a large background, thus minimizing the major problem of incoherent holography. The recording of holograms of fluorescent specimens using temporal, rather than spatial heterodyning has been demonstrated recently with a scanning method.[8]

In this letter, we describe and demonstrate a digital holographic method capable of recording holograms of three-dimensional objects with an arbitrary degree of spatial coherence, and in a single exposure, without any mechanical scan. The coherence of the illumination can be varied as in a conventional microscope by changing the size of the source, a versatility which is important in microscopy where incoherent illumination is preferred if scattering and speckle noise is a problem, but partially coherent illumination is needed for example to visualize phase variations and unstained specimens. The method uses a two-channel interferometric imaging system with a temporal frequency offset to simultaneously encode each object scatterer with a characteristic temporally modulated Fresnel pattern. A CCD sensor samples this spatiotemporal hologram in space and in time simultaneously. The time history of each CCD pixel is filtered about the modulation frequency to extract a two-dimensional array of complex amplitudes representing a single-sideband hologram in which the 3D location of each scatterer is uniquely encoded as a spherical wave. The reconstruction of an image focused on a chosen plane in the object can be done by digital correlation of the holographic data with a wave having a curvature corresponding to that plane. Equivalently, the reconstruction can be obtained by digital correlation with the hologram of a single point object located at the desired depth. This latter scheme has the unique property that the aberrations of the optics, which appear in both the hologram of the object and the hologram of the point source, are canceled out in the reconstruction. The method thus leads to diffraction-limited imaging, independent of the severity of the aberrations of the optics.

The setup used to demonstrate the idea is sketched in Fig. 1. The specimen is illuminated by quasimonochromatic, spatially partially coherent light, and magnified by an objec-

[a]Electronic mail: gindebet@vt.edu



 

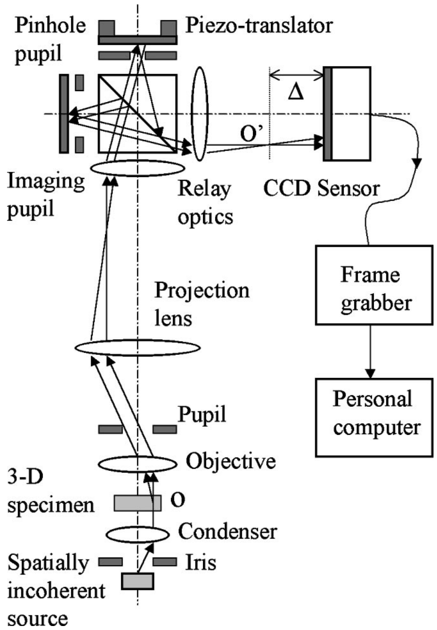


FIG. 1. Sketch of a digital holographic microscope. The saw-tooth-voltage-driven piezo-translator provides a temporal frequency difference between the two arms of the interferometer. The CCD sensor, at a distance Δ from the image plane, samples the hologram in space and in time simultaneously, leading to a on-line, single-sideband Fresnel hologram of the specimen.

tive of focal length $f_o$ with a numerical aperture $\mathrm{NA}_o$, and a projection lens of focal length $f_p$. The magnification is $M_o = f_p/f_o$. A scanning Michelson interferometer incorporating an afocal relay optics can be used for the spatiotemporal encoding, and for the projection on the CCD sensor. One arm of the interferometer is an imaging channel with a pupil matching that of the objective. The other channel has a pinhole as a pupil, and is thus nonimaging. As shown in Fig. 1, a point object $O$ is imaged at $O'$ via channel one, while via channel two, the same point object projects an approximately plane wave front of limited extent centered at $O'$. The CCD sensor is placed at a distance Δ from the image plane, and captures the interference of the two wavelets, which are mutually coherent whether the object is illuminated coherently or incoherently. The interference is a Fresnel pattern having a numerical aperture equal to that of the objective, and a Fresnel number proportional to Δ. The pupils in channels one and two can be expressed as $P_1(\boldsymbol{\rho}) = P_0(\boldsymbol{\rho}) \times \exp(i\pi\lambda\Delta\rho^2)$, and $P_2(\boldsymbol{\rho}) = d(\boldsymbol{\rho})\exp[i(\Omega t+\phi)]$, respectively. $P_1(\boldsymbol{\rho})$ is the usual generalized pupil with defocus Δ,[9] $P_0(\boldsymbol{\rho})$ delimits the boundary of the pupil, and includes the eventual wave front aberrations of the objective, $\phi$ is an arbitrary phase, and $\Omega = 4\pi V/\lambda$ is the Doppler frequency shift generated by a translation of the mirror in channel two at a rate $V$. $P_2(\boldsymbol{\rho})$ is the pinhole pupil of channel two, and can be approximated by a Dirac delta function. The corresponding point-spread functions are $h_{1(2)}(\mathbf{r}) = \int P_{1(2)}(\boldsymbol{\rho}) \times \exp(i2\pi\boldsymbol{\rho}\cdot\mathbf{r})d^2\rho$. With an appropriate size of $d(\boldsymbol{\rho})$, $h_2(\mathbf{r})$ is approximately constant within the support of $h_1(\mathbf{r})$.

The object, with an amplitude transmittance $T(\mathbf{r})$, is illuminated by a quasimonochromatic wave with a transverse coherence function $\Gamma(\mathbf{r})$, and the time history of each pixel of the CCD sensor is recorded and Fourier transformed. At each pixel, the Fourier component at the modulation frequency Ω represents the holographic data at that position. This holographic data has the form $I(\mathbf{r}) = \int\Gamma(\mathbf{r}_1-\mathbf{r}_2)T(\mathbf{r}_1)T^*(\mathbf{r}_2) \times h_1(\mathbf{r}-\mathbf{r}_1)h_2^*(\mathbf{r}-\mathbf{r}_2)d^2\mathbf{r}_1 d^2\mathbf{r}_2$. With incoherent illumination, we have $\Gamma(\mathbf{r}) \sim \delta(\mathbf{r})$ ($\delta$ is a Dirac delta function), and $I_i(\mathbf{r}) \propto \int |T(\mathbf{r}_1)|^2 h_1(\mathbf{r}-\mathbf{r}_1)d^2r_1$. The record is linear in intensity, and thus leads to an imaging process insensitive to phase fluctuations. The previous expression is also valid for self-luminous and fluorescent specimens. With spatially coherent illumination, $\Gamma(\mathbf{r})$ is constant over the extent of the object, and if $h_2$ is a broad, uniform distribution, the holographic record has the form $I_c(\mathbf{r}) \propto \int T(\mathbf{r}_1)h_1(\mathbf{r}-\mathbf{r}_1)d^2r_1$. In this case, the record is linear in amplitude, and the process is capable of imaging phase distributions.

The holographic data can be reconstructed by digital correlation with $h_1(\mathbf{r})$, which can either be constructed analytically, or can be acquired experimentally as the hologram of a single point object. The resulting point-spread function of the reconstructed image has the form $p(\mathbf{r}) = \int h_1(\mathbf{r}')h_1^*(\mathbf{r}'-\mathbf{r})d^2r'$, whether the illumination is coherent or incoherent, and the corresponding transfer function is $P(\boldsymbol{\rho}) = |P_0(\boldsymbol{\rho})|^2$. Clearly, the aberrations of the optics, which are represented by phase distortions in $P_0$, are canceled out, leading to diffraction-limited imaging independently of the optics' aberrations. These features will be explained in more detail and demonstrated elsewhere.

Some experimental results demonstrating the validity of the method were obtained with a standard $504\times485$ pixel CCD camera (i2S model 558). A piezo translator (Burleigh), driven by a saw-tooth voltage, provides a frequency difference between the two arms of the interferometer, and a temporal modulation of the interferogram at ~3.3 Hz. The CCD sensor operated at a rate of 30 frames/s, and the recording time was 50 frames. The light source was an expanded He–Ne laser beam (wavelength 633 nm) passed through a spinning diffuser to render it spatially incoherent. The spectral coherence of a laser is convenient but not necessary. With the interferometer adjusted to zero path difference, the necessary coherence length is determined by the maximum optical path difference through the object, and the excursion of the mirror translation. These are typically of order 10 $\mu$m, so that a source with a linewidth of order 10 nm should be sufficient to produce an interference pattern. For convenience, the experiment was performed with a Mach–Zehnder interferometer and transmitting pupils rather than with a Michelson interferometer and reflecting pupils as shown in Fig. 1, although the latter leads to a more compact design. The imaging pupil is a clear aperture 12 mm diameter, and the nonimaging pupil is a 200 $\mu$m pinhole. The temporally modulated interferogram is simultaneously sampled in space and in time by the CCD sensor, resulting in a on-line, single-sideband hologram in digital form. Figure 2 shows the real part of the hologram (a), and the holographic reconstruction (b) of a 5 $\mu$m pinhole obtained with an objective 10×, effective NA = 0.2, and a projection lens of 16 cm focal length. The relay optics had a magnification of unity (two lenses of focal length 30 cm), and the distance Δ was about 4 cm. Figure 3 shows the holographic reconstruction of the central part of a USAF test chart obtained with the same setup. The reconstruction was obtained by correlation of the hologram with a spherical wave fitted to the hologram of the 5 $\mu$m pinhole. The size of the transverse coherence length of the

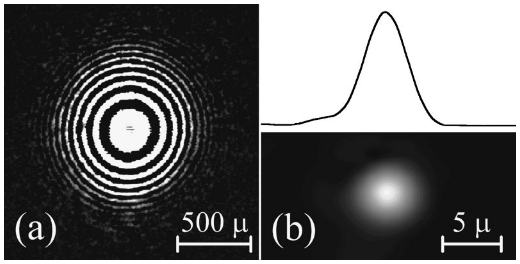


FIG. 2. (a) Hologram of a 5 $\mu$m pinhole (real part) obtained with a 10× objective (NA∼0.2); (b) reconstruction of the 5 $\mu$m pinhole (magnitude displayed with interpolation) using a spherical wave fitted to the hologram shown in (a).

illumination was about 25 $\mu$m. With a broader source, and thus less spatial coherence, the noise is reduced, but so is the contrast of the pattern, thus requiring a detector with larger dynamic range. The resolution of the reconstruction is limited partly by the numerical aperture of the objective, and partly by the size of the CCD pixels ($12.7\times 9.8\,\mu$m).

A detailed description of the imaging property of the method will appear elsewhere, but it is useful to briefly compare the properties of the reconstructed image with those of an image obtained directly with the same objective and projection optics. The optical transfer function of the direct incoherent imaging system has the usual quasiconical shape[9] tapered down to zero at the cutoff frequency $\nu_i = 2\mathrm{NA}_o/\lambda$. The aberrations of the objective further reduce the contrast of the higher spatial frequencies.[9] That of the direct coherent imaging process is flat up to the cutoff $\nu_c = \nu_i/2$. Aberrations have more severe consequences, as they directly affect the phase of the spatial frequencies, often resulting in high contrast coherent artifacts. In the holographic process, the transfer function is flat up to the same cutoff frequency $\nu_c$ for both the coherent and incoherent holograms, and as already mentioned, the aberrations can be canceled out by reconstruction with the hologram of a point source recorded with the same setup. The point-spread function of the direct coherent image is $\mathrm{PSF}_c = 2J_1(X)/X$, $X = 2\pi r(\mathrm{NA}_o)/\lambda$, while that of the direct incoherent image is $\mathrm{PSF}_i = |\mathrm{PSF}_c|^2$. The point-spread function of the holographic reconstruction is $\mathrm{PSF}_h = 2J_1(X)/X$, whether the imaging process is linear in intensity or in amplitude. A more important difference is that, although direct coherent imaging is linear in amplitude, the phase information is lost once the image is recorded on a quadratic detector, unless an interferometric detection (such as, e.g., Zernike phase contrast), is used. The holographic reconstruction, on the other hand, contains the phase information. This opens up vast possibilities for *a posteriori* processing of the information, some examples of which will be shown elsewhere. It is interesting to note that the resolution of the holographic image is independent of the defocus distance $\Delta$. This distance, however, determines the Fresnel number of the encoding pattern. The magnification of the relay optics and the Fresnel number are design parameters that can be used to match the hologram size with the resolution of the CCD.

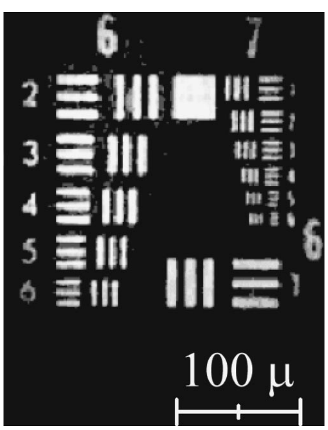


FIG. 3. Reconstruction of the central part of a USAF test chart (magnitude) recorded with spatially partially coherent illumination, and the same objective and magnification as in Fig. 2. The smallest feature has a spatial frequency of 228 lines/mm.

In summary, we have described and demonstrated experimentally a digital holographic method in which the hologram is recorded in the spatial and temporal domains simultaneously. Using temporal heterodyning rather than spatial heterodyning, one directly obtains an on-line, single-sideband hologram with relaxed demand on the spatial bandwidth of the detector, and no real need for spatially coherent illumination. The transverse spatial coherence can be varied at will, and the longitudinal coherence length of the radiation must only be larger than the maximum optical path difference in the interferometer. The method circumvents most of the drawbacks of both coherent and incoherent holography, namely speckle noise and low signal-to-background ratio, respectively. It is suitable for recording in a single exposure, speckle-free holograms of rough, scattering objects, holograms of phase distributions, as well as holograms of self-luminous and fluorescent specimens. A detailed analysis of these attributes, and their demonstration, will appear elsewhere.

[1] R. J. Collier, C. B. Burckhardt, and L. H. Lin, *Optical Holography* (Academic, New York, 1971).
[2] E. Cuche, F. Bevilaqua, and C. Depeursinge, Opt. Lett. **5**, 291 (1999).
[3] D. Gabor, Nature (London) **161**, 777 (1948); Proc. R. Soc. London, Ser. A **197**, 454 (1949); Proc. A. Soc. London, Ser. B **64**, 449 (1951).
[4] E. N. Leith and J. Upatnieks, J. Opt. Soc. Am. **52**, 1123 (1962); **53**, 1377 (1963); **54**, 1295 (1964).
[5] E. N. Leith and J. Upatnieks, J. Opt. Soc. Am. **55**, 569 (1965); R. V. van Ligten and H. Osterberg, Nature (London) **211**, 282 (1966).
[6] *Laser Speckle and Related Phenomena*, edited by J. C. Dainty (Springer, Berlin, 1984).
[7] P. Hariharan and G. G. Sing, J. Opt. Soc. Am. **49**, 732 (1959); M. V. R. K. Murty, *ibid.* **54**, 1187 (1964); A. Lohmann, *ibid.* **55**, 1555 (1965); L. Metz, *Transformations in Optics* (Wiley, New York, 1965).
[8] B. W. Schilling, T.-C. Poon, G. Indebetouw, B. Storie, K. Shinoda, Y. Suzuki, and M. H. Wu, Opt. Lett. **22**, 1506 (1997).
[9] J. W. Goodman, *Introduction to Fourier Optics* (McGraw–Hill, New York, 1968).